

This discussion paper is/has been under review for the journal Atmospheric Chemistry and Physics (ACP). Please refer to the corresponding final paper in ACP if available.

Sensitivity of simulated climate to latitudinal distribution of solar insolation reduction in SRM geoengineering methods

A. Modak and G. Bala

Divecha Centre for Climate Change & Centre for Atmospheric and Oceanic Sciences, Indian Institute of Science, Bangalore – 560 012, India


Received: 15 July 2013 – Accepted: 14 September 2013 – Published: 1 October 2013

Correspondence to: A. Modak (amatcaos@caos.iisc.ernet.in)

Published by Copernicus Publications on behalf of the European Geosciences Union.

25387

Abstract

Solar radiation management (SRM) geoengineering has been proposed as a potential option to counteract climate change. We perform a set of idealized geoengineering simulations to understand the global hydrological implications of varying the latitudinal distribution of solar insolation reduction in SRM methods. We find that for a fixed total mass of sulfate aerosols (12.6 Mt of SO₄), relative to a uniform distribution which mitigates changes in global mean temperature, global mean radiative forcing is larger when aerosol concentration is maximum at the poles leading to a warmer global mean climate and consequently an intensified hydrological cycle. Opposite changes are simulated when aerosol concentration is maximized in the tropics. We obtain a range of 1 K in global mean temperature and 3% in precipitation changes by varying the distribution pattern: this range is about 50% of the climate change from a doubling of CO₂. Hence, our study demonstrates that a range of global mean climate states, determined by the global mean radiative forcing, are possible for a fixed total amount of aerosols but with differing latitudinal distribution, highlighting the need for a careful evaluation of SRM proposals. 

1 Introduction

Atmospheric concentrations of the greenhouse gases (GHGs) such as carbon dioxide (CO₂), methane (CH₄) and nitrous oxide (N₂O) have been increasing since pre-industrial periods primarily because of fossil fuel use and land-use change (IPCC, 2007). Their increase has the potential to cause long term climate change by altering the planetary radiation budget. To moderate future climate change and its impacts, several geoengineering proposals have been made recently. By definition, geoengineering is an intentional large-scale manipulation of the environment, particularly intended to counteract the undesired consequences of anthropogenic climate change (Keith, 2000).

25388

Proposed geoengineering methods are classified into two main groups: Solar Radiation Management (SRM) methods and Carbon dioxide Removal (CDR) methods (Shepherd et al., 2009). In the first approach, the amount of solar absorption by the planet is reduced by artificially enhancing the planetary albedo so that the reduced insolation compensates the radiative forcing due to rising GHGs. Some proposed methods are injecting sulfate aerosols in the stratosphere (Budkyo, 1982; Crutzen, 2006; Wigley, 2006) and placing space based sun shields in between the Sun and the Earth (Early, 1989). CDR methods propose to accelerate the removal of CO₂ from the atmosphere and thus they deal with the root cause of global warming (The Royal Society, 2009).

Past climate modeling studies have modeled the effects of space-based SRM methods by reducing the solar constant (Govindasamy and Caldeira, 2000; Matthews and Caldeira, 2007; Caldeira and Wood, 2008; Lunt et al., 2008) or modeled the effects of stratospheric aerosol methods (Robock et al., 2008; Rasch et al., 2008a, b; Heckendorn et al., 2009; Jones et al., 2010). It has been shown (Bala et al., 2008) that SRM geoengineering would lead to a weakening of the global water cycle when the global mean temperature change is mitigated exactly. Further, it has been shown (Robock et al., 2008; Ricke et al., 2010) that the level of compensation will vary with residual changes larger in some regions than others. Therefore, some recent studies (Ban-Weiss and Caldeira, 2010; MacMartin et al., 2012) determine an optimal reduction in solar radiation in both space and time so the geoengineered world is more similar to the control climate while other studies (Irvine et al., 2010; Ricke et al., 2010) analyze the effect of different levels of uniform SRM forcing on regional climate response. Ban-Weiss and Caldeira (2010) vary both the amount and latitudinal distribution of aerosols to mitigate either the zonally averaged changes in surface temperature or the water budget. However, a simple and clear understanding of the effects of varying the latitudinal distribution of aerosols and hence solar insolation reduction (e.g. more concentration in the tropics or high latitudes) on the hydrological cycle and surface temperature is lacking. In this study, we perform multiple idealized SRM geoengineering simulations

25389

with constant total amount of sulfate aerosols but with systematically varying latitudinal distribution.

We caution that our simulations are highly idealized and they are not meant to represent realistic latitudinal distribution of aerosols in geoengineering scenarios. Rather, they are designed to elucidate the fundamental properties of the climate system when the latitudinal distribution of aerosols and hence solar insolation reduction is systematically altered. We believe that our study should be considered as complementary to a previous work (Ban-Weiss and Caldeira, 2010), because not only we vary the latitudinal distribution of aerosols but we also provide a constraint by fixing the total amount of aerosols which facilitates a clear insight on the effects of varying the latitudinal distribution of aerosols.

2 Model and experiments

We used the atmospheric general circulation model, CAM3.1 developed at the National Center for Atmospheric Research (NCAR) (Collins et al., 2004). It is coupled to the land model CLM3.0 and to a slab ocean model (SOM) with a thermodynamic sea ice model to represent the interactions with the ocean and sea ice components of the climate system. The model can be also configured with prescribed sea surface temperature and sea ice fraction. The horizontal resolution is 2° latitude and 2.5° longitude and the model has 26 vertical levels and the top of the model (TOM) is at 3 hPa.

We performed two sets of simulations: (1) fixed-SST (sea surface temperature) simulations to estimate the radiative forcing which is measured as the net radiative flux change at the top of the atmosphere (Hansen et al., 1997). (2) The other set include the SOM simulations to study the climate change. For both set of simulations, fixed-SST and SOM, we performed twelve cases: a control (1 × CO₂), doubled CO₂ climate (2 × CO₂) and ten geoengineering simulations each with differing latitudinal distribution of sulfate aerosol concentrations but with fixed total amount. The concentration of atmospheric CO₂ in 1 × CO₂ is 390 ppm and is 780 ppm in 2 × CO₂ and geoengineering

25390

simulations. The concentrations of other greenhouse gases are kept constant in all simulations. The background sulfate aerosol amount in this version of the model is 1.38 Mt SO_4 . The fixed-SST simulations lasted for 30 yr and the last 20 yr are used to calculate the radiative forcing. The SOM simulations lasted for 60 yr and the last 30 yr are used for climate change analysis since all SOM simulations reach a near-equilibrium climate state in approximately 25 yr.

In each of the geoengineering simulations (Table 1, Fig. 1a) aerosol mass is added to the model background concentration at the TOM as was done in a recent study (Ban-Weiss and Caldeira, 2010). As in Ban-Weiss and Caldeira (2010), this additional sulfate is prescribed and hence it is not transported around. However, in contrast to Ban-Weiss and Caldeira (2010), we introduce the constraint that the total amount of aerosol is constant (12.6 Mt SO_4) while latitudinal distributions are varied. Since aerosols are prescribed at TOM, the effect is essentially equivalent to making latitudinal changes to the solar constant. Sulfate aerosol particle size is prescribed and is assumed to be log-normally distributed with dry median radius $\approx 0.05 \mu\text{m}$ and geometric standard deviation ≈ 2.0 (as used in a geoengineering scenario in a previous study, Rasch et al., 2008b). The aerosol indirect effects are not modeled and aerosol loadings for other species like sea-salt, soil dust, black and organic carbon are unchanged in each of the simulations.

Besides a simulation with uniform aerosol concentration, our geoengineering simulations can be grouped into two categories: (1) Three “Tropics” simulations with maximum aerosol concentrations at the equator and (2) Six “Polar” cases with maximum concentrations at the poles. The latitudinal distribution of the stratospheric sulfate aerosol concentration are developed using the expression:

$$Q(\varphi) = a + b\cos(\varphi) \quad (1)$$

where Q is the concentration of the additional mass of sulfate aerosols, a and $b\cos(\varphi)$ are the uniform and non-uniform components of the distributions and φ represents the latitude. Both a and b are varied to obtain various distributions of concentrations

25391

(Table 1, Fig. 1a). However, when Q is integrated over the sphere, the result is 12.6 Mt in all the cases. Our choice of 12.6 Mt for Q is dictated by the uniform distribution case which had near-zero global mean temperature change relative to the control case.

3 Results

3.1 Global mean temperature and precipitation response

We find that the radiative forcing for doubling the atmospheric CO_2 ($2 \times \text{CO}_2$) to be 3.5 W m^{-2} while the global mean surface temperature rise is about 2.1 K and the precipitation increase is about 4.3 % (i.e. $\approx 2 \% \text{ K}^{-1}$) in agreement with previous studies using the same model (Rasch et al., 2008b; Bala et al., 2009). The slopes in Fig. 1c and 1d indicate a climate sensitivity of $0.53 \text{ K (Wm}^{-2}\text{)}^{-1}$ and precipitation sensitivity (% change in precipitation for unit change in radiative forcing) of $1.53 \% (\text{Wm}^{-2}\text{)}^{-1}$ respectively, values that are similar to Bala et al. (2009).

The slight warming in the geoengineering case where forcing is close to zero (Fig. 1c) is because of the CO_2 physiological forcing (Betts et al., 2007; Cao et al., 2010) which is not counteracted by a decrease in solar flux. CO_2 physiological forcing refers to the direct physiological response of plants to elevated CO_2 : the plant stomata open less widely and thus decrease the canopy transpiration which in turn reduces evapotranspiration and causes surface warming. Therefore, in the zero radiative forcing case where CO_2 radiative forcing is countered by the reduction in solar radiation, the CO_2 -physiological forcing leads to a slight warming.

In agreement with past studies (e.g. Lunt et al., 2008; Bala et al., 2008), we find that in the geoengineering scenario with uniform distribution of aerosol there is a decline in precipitation though the temperature change is completely mitigated (Fig. 1b). This occurs because of differing fast response in precipitation for solar and CO_2 -forcing (Allen and Ingram, 2002; Bala et al., 2008, 2009; Andrews et al., 2009). CO_2 -forcing heats the troposphere, increases the vertical stability and thus leads to precipitation suppres-

25392

sion (Cao et al., 2012). In contrast, solar forcing tends to heat the atmosphere only slightly causing much smaller change in precipitation. Therefore, in a geoengineered world the precipitation suppression caused by CO₂-forcing is not mitigated by the specified amount of solar forcing which mitigates temperature change. This suppression of precipitation is simulated in all geoengineering simulations (the regression line does not pass through the origin in Fig. 1b). Therefore the precipitation change in any geoengineering simulation can be inferred from the linear relationship between changes in precipitation and temperature changes and the fast response component.

Our geoengineering simulations with varying aerosol distributions indicate a linear relationship between the global mean surface temperature change and the precipitation change (Fig. 1b). The regression lines do not pass through the origin which implies that none of the distribution can mitigate global mean temperature and precipitation simultaneously. Though the total amount of aerosols in each of the geoengineering simulation is fixed, we obtain a range of 1 K (residual cooling of 0.3 K for the Tropics3 case to residual warming of 0.7 K for the Polar6 case) in global mean temperature and 3 % (residual drying of 2 % for Tropics3 case to residual increase of 1 % for the Polar6 case) in precipitation changes which are about 50 % or more of the changes that result from doubling of CO₂. This indicates that a range of climate states are possible for a constant amount of aerosols.

As the polar maximum of the aerosol concentration increases the global mean temperature increases with concomitant increase in global mean precipitation as implied by the linear relationship in Fig. 1b. One of the polar maximum SRM simulations (Polar3) almost offsets the changes in global mean precipitation but it has a residual warming of 0.4 °C. Our results are broadly in agreement with other modeling studies: in an Arctic geoengineering study (Caldeira and Wood, 2008) with reduced solar constant only over arctic, residual global mean warming and enhancements of global precipitation are found.

In contrast, as magnitude of the tropical maximum concentration increases both global mean temperature and precipitation decreases. One of the Tropics cases (Trop-

25393

ics1) where the temperature change is nearly zero shows a reduction in the global mean precipitation. The reduction in precipitation in our “Tropics” simulations are consistent with observed decline in precipitation over land, runoff and river discharge into the ocean following the tropical volcanic eruption Mount Pinatubo (15° N) in 1991 (Trenberth and Dai, 2007). **Interestingly, we find that in none of the geoengineering scenarios changes in global mean surface temperature and precipitation can be mitigated simultaneously over either land or ocean.** We also notice that the hydrological sensitivity (% change in precipitation per unit change in temperature) is almost same over both land and ocean (Fig. 1b). Here, we have defined the hydrological sensitivity over land (ocean) as the ratio of change in land (ocean) averaged precipitation to change in land (ocean) averaged surface temperature.

We find that the prescribed aerosols with different latitudinal distributions along with doubled CO₂ concentrations (geoengineering simulations) lead to different global mean forcings (Fig. 1c and d). Since there are linear relationships between radiative forcing and the changes in global mean temperature (Fig. 1c) and between temperature and precipitation changes (Fig. 1b), we find a linear relationship between radiative forcing and precipitation changes (Fig. 1d). The Polar geoengineering scenarios have positive residual radiative forcing while the Tropics scenarios have negative residual forcing because solar forcing is less effective over the poles relative to the tropics (Fig. 1c). This is further confirmed in Fig. 2 which shows that the Polar cases have smaller increase in planetary albedo compared to the Tropics cases. The radiative forcing associated with planetary albedo changes drive the temperature changes and thus the Polar cases have lower albedo changes relative to the uniform case and hence are warmer and wetter while opposite is true for Tropics cases.

The variation of global mean surface temperature and precipitation with global mean radiative forcing (Fig. 1c and 1d) shows that as the maximum aerosol concentration over the poles increases (Polar1 to Polar6) the residual forcing increases and hence the global mean temperature and precipitation increase. Similarly, as the maximum

25394

aerosol concentration over the equator increases (Tropics1 to Tropics3), an opposite variation is noticed.

The root mean square difference (RMSD) of the geoengineering simulations with respect to the control case, normalized by the spatial standard deviation in the control scenario shows that the RMSD in temperature increases as the maximum concentration of aerosols at the poles increases and the RMSD in precipitation increases as tropical maximum is increased (Fig. 3). We normalize RMSD by standard deviation in the control scenario so the RMSD between a geoengineered and a control world can be compared to the regional variations in the control simulation. Figure 3a shows the ratio of spatial RMSD and standard deviation of the control simulation while the ratio of zonal mean RMSD and standard deviation is shown in Fig. 3b. In case of spatial RMSD the spread is more, 0.40 to 1.4 for surface temperature and 0.25 to 0.40 for precipitation. In case of RMSD in zonal means, the spread is relatively less: 0.30 to 0.95 for surface temperature and 0.27 to 0.38 for precipitation. The uniform case has the least distance from the origin in Fig. 3, suggesting that it has the least RMSD if the objective is to minimize RMSD in both temperature and precipitation simultaneously.

3.2 Precipitation and temperature response in Tropics and Poles

The change in zonal-mean surface temperature between the geoengineering cases and the control case ($1 \times \text{CO}_2$) show, similar to changes in global annual mean values, a monotonic increase at each latitude with increased polar weighting (Fig. 4a). We notice a similar monotonic increase in zonal-mean land and zonal-mean ocean surface temperature (Fig. 5a and 5b). Further, we find that almost all geoengineering simulation show residual high latitude warming. In the Tropics cases, we find smaller residual warming in the high latitudes and cooler tropics. Similar to temperature changes, the change in zonal-mean precipitation between the geoengineering cases and the control case show a monotonic increase at each latitude with increased polar weighting (Figs. 4b, 5c and 5d). We find large changes in precipitation in the tropics which is likely to be seen as shifts in the intertropical convergence zone (ITCZ) but closer examina-

25395

tion (Fig. 6) shows that the position of ITCZ remains the same in all the cases and the monotonic increase in precipitation with poleward weighting is clearly seen. The changes in zonal mean precipitation minus evaporation (water budget) are similar to changes in zonal mean precipitation (Figs. 4c, 5e and 5f).

Figure 7 shows the spatial pattern of radiative forcing in selected simulations: $2 \times \text{CO}_2$, Uniform, Polar3, Tropics1, Polar6 and Tropics3 cases. We notice that the radiative forcing in the $2 \times \text{CO}_2$ case is significant over the whole globe but not significant in most regions in the geoengineering cases. The radiative forcing is positive in most locations in case of Polar cases. In the Tropics cases, the forcing is negative in the tropical regions and positive in polar regions.

In the $2 \times \text{CO}_2$ case, both temperature and precipitation changes are large and significant over the whole globe (Fig. 8). The temperature increase over poles is much larger than in the tropics, in agreement with previous studies (Caldeira and Wood, 2008; Lun-tet et al., 2008; Matthews and Caldeira, 2007; Robocket al., 2008; Rasch et al., 2008b). The uniform geoengineering case (Uniform) shows mitigation in the temperature with reduced precipitation relative to $1 \times \text{CO}_2$. This is because of the different nature of the CO_2 forcing and solar forcing: solar forcing is larger in the tropics and smaller in the poles whereas the CO_2 forcing is uniform over the whole globe. In Polar3 case, the change in precipitation is largely mitigated but there is significant warming over large regions. However, temperature is largely mitigated in Tropics1 but there is decrease in precipitation relative to the uniform distribution case. The last four panels of Fig. 8 shows the extreme cases; the case with largest polar weighting (Polar6) significantly warms the planet while the case with largest tropical weighting (Tropics3) overcools the planet with large reduction in precipitation. The seasonal variations in residual temperatures mostly occur in the high latitudes with stronger response in the winter and weaker response in the summer (Fig. 9) following the seasonal cycle of radiative forcing (Fig. 7; right panels). The magnitude of seasonal variations in precipitation response is large in the tropics in the geoengineering cases but with reduced intensity compared to the $2 \times \text{CO}_2$ case.

4 Discussion and conclusions

In this study, we find that when the latitudinal distribution of sulfate aerosols is altered the global mean radiative forcing changes which leads to changes in surface temperature as indicated by the climate sensitivity of the model (Fig. 1c). Consequent changes in global mean precipitation are simulated as dictated by the hydrological sensitivity of the model (Fig. 1b). We also observe a similar monotonic increase in precipitation intensity as the maximum aerosol concentration over the poles increases (Fig. 10). The increases are of the order of 10 % for low intensity (5th percentile) and 2–3 % for large intensity (99th percentile) between the extreme cases (Tropics3 and Polar6). In order to confirm that global mean radiative forcing is sufficient to infer the global mean climate change we performed four additional geoengineering simulations with total amount of aerosols varied (10 Mt, 11 Mt, 13 Mt and 14 Mt) for the uniform distribution case. We find that the global mean temperature and precipitation changes follow the changes in global mean forcing (Fig. 11) for this set of simulations too.

In agreement with earlier studies (e.g. Bala et al., 2008), we find that both temperature and precipitation changes cannot be mitigated simultaneously in all geoengineering simulations considered in this study (that is, even with non-uniform distribution of solar insolation reduction). The latitudinal distribution which offsets the warming leads to a drier climate while the distribution which offsets the precipitation results in a relatively warmer world (note that Bala et al. (2008) used a uniform solar insolation reduction). For a fixed total amount of aerosols but with different latitudinal distribution it is possible to achieve a range of global mean radiative forcing and thus a range of climate states.

Our findings should be viewed in the light of the limitations and uncertainties involved in this study. Our simulations are highly idealized as we have prescribed sulfate aerosol (to reduce the solar insolation) instead of injecting and transporting them. We have prescribed a fixed particle size distribution but particle size distribution would evolve with time and is shown to be important in precisely estimating the effects on different climate

25397

variables (Rasch et al., 2008b). Some modeling studies (Robock et al., 2008) have injected aerosol precursors into to the stratosphere with fixed particle size distribution while other studies (Heckendorn et al., 2009; Pierce et al., 2010; Niemeier et al., 2010; Hommel and Graf, 2011; English et al., 2012) have demonstrated the importance of including the microphysics of particle growth. Further, we have focused our investigation primarily on global mean climate while several other studies (e.g. Robock et al., 2008; Irvine et al., 2010; Ricke et al., 2010) focused on regional disparities.

In this study, we have not considered the consequences of sulfate aerosol chemistry on the ozone layer (Tilmes et al., 2009). Our model lacks a dynamic ocean and sea ice components and the effects of deep ocean circulation are not modeled here. However, we believe our results on temperature and precipitation is so fundamental that they would be unchanged when additional components and feedbacks are included.

In summary, for a fixed total mass of aerosols, we find that the global mean climate is warmer and wetter when aerosol concentration is maximum over the poles relative to the uniform distribution case (which mitigates global mean temperature change) because the global mean residual radiative forcing is positive in these cases when compared to the uniform case. The opposite is true when aerosol concentration is maximum in the tropics. Further, our study clearly indicates that knowledge of global mean radiative forcing, not the details of latitudinal distribution of aerosols, is sufficient to infer the global mean climate change.

Acknowledgements. Financial support for A. Modak was provided by the Divecha Centre for Climate Change, Indian Institute of Science. We thank the Supercomputer Education and Research Centre, Indian Institute of Science for providing the computational resources.

References

Allen, M. R. and Ingram, W. J.: Constraints on future changes in climate and the hydrologic cycle, *Nature*, 419, 224–232, doi:10.1038/nature01092, 2002.

25398

- Andrews, T., Forster, P. M., and Gregory, J. M.: A surface energy perspective on climate change, *J. Climate.*, 22, 2557–2570, doi:10.1175/2008JCLI2759.1, 2009.
- Bala, G., Caldeira K., and Nemani, R.: Fast versus slow response in climate change: implications for the global hydrological cycle, *Clim. Dynam.* 35, 423–434, doi:10.1007/s00382-009-0583-y, 2009.
- 5 Bala, G., Duffy P. B., and Taylor, K. E.: Impact of geoengineering schemes on the global hydrological cycle, *P. Natl. Acad. Sci. USA*, 105, 7664–7669, doi:10.1073/pnas.0711648105, 2008.
- Ban-Weiss, G. A. and Caldeira, K.: Geoengineering as an Optimization Problem, *Environ. Res. Lett.*, 5, 034009, doi:10.1088/1748-9326/5/3/034009, 2010.
- 10 Betts, R. A., Boucher, O., Matthew, C., Cox, P. M., Falloon, P. D., Gedney, N., Hemming, D. L., Huntingford, C., Jones, C. D., Sexton, D. M. H., and Webb, M. J.: Projected increase in continental runoff due to plant responses to increasing carbon dioxide, *Nature*, 448, 1037–1041, doi:10.1038/nature06045, 2007.
- 15 Budkyo, M. I.: *The Earth's Climate Past and Future*, Academic, 1982.
- Caldeira, K. and Wood, L.: Global and Arctic climate engineering: Numerical model studies, *Philos. T. Roy. Soc. A*, 366, 4039–4056, doi:10.1098/rsta.2008.0132, 2008.
- Cao, L., Bala, G., Caldeira, K., Nemani, R., and Ban-Weiss, G. A.: Importance of carbon dioxide physiological forcing to future climate change, *P. Natl. Acad. Sci. USA*, 107, 9513–9518, doi:10.1073/pnas.0913000107, 2010.
- 20 Cao, L., Bala, G., and Caldeira, K.: Climate response to changes in atmospheric carbon dioxide and solar irradiance on the time scale of days to weeks, *Environ. Res. Lett.*, 7, 034015, doi:10.1088/1748-9326/7/3/034015, 2012.
- Collins, W. D., Rasch, P. J., Boville, B. A., Hack, J. J., McCaa, J. R., Williamson, D. L., Kiehl, J. T., Briegleb, B., Bitz, C., Lin, S.-J., Zhang, M., and Dai, Y.: Description of the NCAR community atmosphere model (CAM 3.0) NCAR Tech. Rep. NCAR/TN-464+STR National Center for Atmospheric Research Boulder CO 226 pp., 2004.
- 25 Crutzen, P. J.: Albedo enhancement by stratospheric sulfur injections: A contribution to resolve a policy dilemma?, *Climatic Change*, 77, 211–220, doi:10.1007/s10584-006-9101-y, 2006.
- 30 Early, J. T.: Space-based solar shield to offset greenhouse effect, *JBIS-J. Brit. Interpla.*, 42, 567–569, 1989.

25399

- English, J. M., Toon, O. B., and Mills, M. J.: Microphysical simulations of sulfur burdens from stratospheric sulfur geoengineering, *Atmos. Chem. Phys.*, 12, 4775–4793, doi:10.5194/acp-12-4775-2012, 2012.
- Govindasamy, B. and Caldeira, K.: Geoengineering Earth's radiation balance to mitigate CO₂-induced climate change, *Geophys. Res. Lett.*, 27, 2141–2144, 2000.
- 5 Hansen, J., Sato, M., and Ruedy, R.: Radiative forcing and climate response, *J. Geophys. Res.*, 102, 6831–6864, 1997.
- Heckendorn, P., Weisenstein, D., Fueglistaler, S., Luo, B. P., Rozanov, E., Schraner, M., Thomason, L. W., and Peter, T.: The impact of geoengineering aerosols on stratospheric temperature and ozone, *Environ. Res. Lett.*, 4, 045108, doi:10.1088/1748-9326/4/4/045108, 2009.
- 10 Hommel, R. and Graf, H. F.: Modelling the size distribution of geoengineered stratospheric aerosols, *Atmos. Sci. Lett.*, 12, 168–175, doi:10.1002/asl.285, 2011.
- Irvine, P. J., Ridgwell, A., and Lunt, D. J.: Assessing the regional disparities in geoengineering impacts, *Geophys. Res. Lett.*, 37, L18702, doi:10.1029/2010GL044447, 2010.
- 15 IPCC 2007 Climate Change 2007: The Physical Science Basis Contribution of Working Group 1 to the Fourth Assessment Report of the Intergovernmental Panel on Climate Change ed Solomon, S., Qin, D., Manning, M., Chen, Z., Marquis, M., Averyt, K. B., Tignor, M., and Miller, H. L.: (Cambridge & New York: Cambridge University Press) 996 pp., 2007.
- Jones, A., Haywood, J., Boucher, O., Kravitz, B., and Robock, A.: Geoengineering by stratospheric SO₂ injection: results from the Met Office HadGEM2 climate model and comparison with the Goddard Institute for Space Studies ModelE, *Atmos. Chem. Phys.*, 10, 5999–6006, doi:10.5194/acp-10-5999-2010, 2010.
- 20 Keith, D. W.: Geoengineering the climate: history and prospect, *Annu. Rev. Energ. Env.*, 25, 245–284, 2000.
- 25 Lunt, D. J., Ridgwell, A., Valdes, P. J., and Seale, A.: 'Sunshade world': a fully coupled GCM evaluation of the climatic impacts of geoengineering, *Geophys. Res. Lett.*, 35, L12710, doi:10.1029/2008GL033674, 2008.
- MacMartin, D. G., Keith, D. W., Kravitz, B., and Caldeira, K.: Management of trade-offs in geoengineering through optimal choice of non-uniform radiative forcing, *Nature Climate Change*, 3, 365–368, doi:10.1038/nclimate1722, 2012.
- 30 Matthews, H. D. and Caldeira, K.: Transient climate-carbon simulations of planetary geoengineering, *P. Natl. Acad. Sci. USA*, 104, 9949–9954, doi:10.1073/pnas.0700419104, 2007.

25400

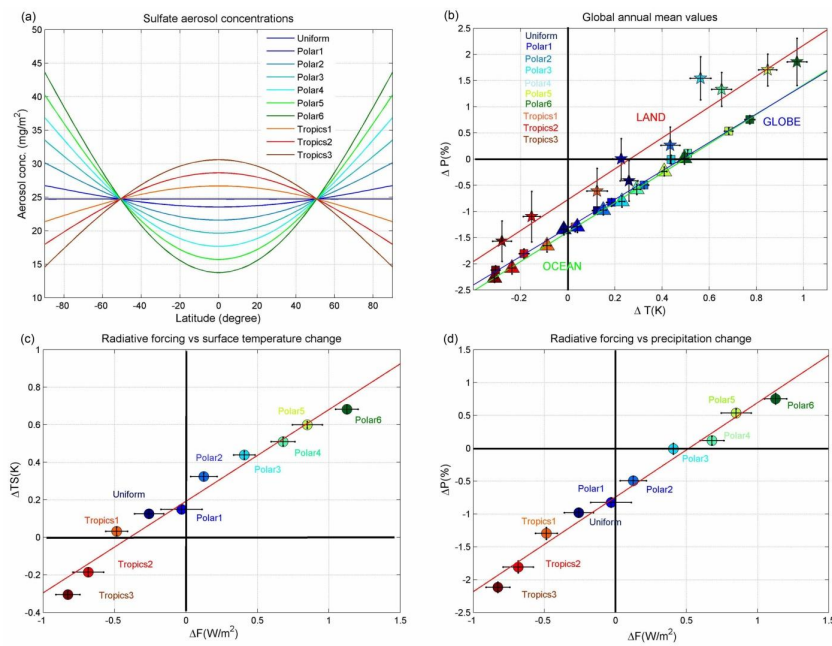
- Niemeier, U., Schmidt, H., and Timmreck, C.: The dependency of geoengineered sulfate aerosol on the emission strategy, *Atmos. Sci. Lett.*, 12, 189–194, doi:10.1002/asl.304, 2010.
- Pierce, J. R., Weisenstein, D. K., Heckendorn, P., Peter, T., and Keith, D. W.: Efficient formation of stratospheric aerosol for climate engineering by emission of condensable vapor from aircraft, *Geophys. Res. Lett.*, 37, L18805, doi:10.1029/2010GL043975, 2010.
- Rasch, P. J., Tilmes, S., Turco, R. P., Robock, A., Oman, L., Chen, C. C., Stenchikov, G. L., and Garcia, R. R.: An overview of geoengineering of climate using stratospheric sulphate aerosols, *Philos. T. Roy. Soc. A*, 366, 4007–4037, doi:10.1098/rsta.2008.0131, 2008a.
- Rasch, P. J., Crutzen, P. J., and Coleman, D. B.: Exploring the geoengineering of climate using stratospheric sulfate aerosols: The role of particle size, *Geophys. Res. Lett.*, 35, L02809, doi:10.1029/2007GL032179, 2008b.
- Ricke, K. L., Morgan, M. G., and Allen, M. R.: Regional climate response to solar-radiation management, *Nat. Geosci.*, 3, 537–541, 2010.
- Robock, A., Oman, L., and Stenchikov, G. L.: Regional climate responses to geoengineering with tropical and Arctic SO₂ injections, *J. Geophys. Res.*, 113, D16101, doi:10.1029/2008JD010050, 2008.
- Shepherd, J., Caldeira, K., Haigh, J., Keith, D., Launder, B., Mace, G., MacKerron, G., Pyle, J., Rayner, S., Redgwell, C., and Watson, A.: *Geoengineering the climate: science, governance and uncertainty*, The Royal Academy, 2009.
- Tilmes, S., Garcia, R. R., Kinnison, D. E., Gettelman, A., and Rasch, P. J.: Impact of geoengineered aerosols on the troposphere and stratosphere, *J. Geophys. Res.*, 114, D12305, doi:10.1029/2008JD011420, 2009.
- Trenberth, K. E. and Dai, A.: Effects of Mount Pinatubo volcanic eruption on the hydrological cycle as an analog of geoengineering, *Geophys. Res. Lett.*, 34, L15702, doi:10.1029/2007GL030524, 2007.
- Wigley, T. M. L.: A combined mitigation/geoengineering approach to climate stabilization, *Science*, 314, 452–454, doi:10.1126/science.1131728, 2006.

25401

Table 1. Description of different geoengineering experiments. Total additional mass is 12.6 Mt SO₄ in all the geoengineering simulations but the distribution varies.

Name of the Experiments	<i>a</i> (mg m ⁻²)	<i>b</i> (mg m ⁻²)	Total Mass from uniform component (Mt)	Total Mass from non-uniform component (Mt)	Total Mass (Mt)
Uniform	24.70	–	12.60	–	12.60
Polar1	23.52	3.19	12.00	0.60	12.60
Polar2	21.56	8.55	11.00	1.60	12.60
Polar3	19.60	13.89	10.00	2.60	12.60
Polar4	17.64	19.22	9.00	3.60	12.60
Polar5	15.68	24.56	8.00	4.60	12.60
Polar6	13.72	29.90	7.00	5.60	12.60
Tropics1	26.66	–5.34	13.60	–1.00	12.60
Tropics2	28.62	–10.67	14.60	–2.00	12.60
Tropics3	30.58	–16.02	15.60	–3.00	12.60

25402



25403

Fig. 1. (a) Latitudinal profiles of sulfate aerosol concentration in the SRM geoengineering experiments. Polar1–6 have maximum concentration over the poles and Tropics1–3 have maximum at the equator. (b) Surface temperature change (K) vs. precipitation change (%) relative to the 1xCO₂ case from slab ocean simulations (global mean values – squares, land mean values – stars, ocean mean values – triangles). There is warming in all Polar cases relative to the uniform case and a concomitant increase in precipitation. Opposite is the case for Tropics cases. None of the regression lines pass through origin; temperature and precipitation cannot be mitigated simultaneously. In the case of land and ocean, ΔTS and ΔP represent the averages over the respective domain. (c) Radiative forcing (RF) vs. surface temperature change. Polar cases have larger forcing relative to the uniform case and hence are warmer while opposite is true for Tropics cases. (d) Radiative forcing vs. % precipitation change. Precipitation increases with residual RF (i.e. with increase in polar weighting) while decreases with increase in tropical weighting. In (b), (c) and (d) the horizontal and vertical bars represent the standard error of the respective variables which are calculated from the last 30 yr of 60 yr SOM simulations while in case of radiative forcing it is calculated from the last 20 yr of 30 yr fixed-SST simulations.

25404

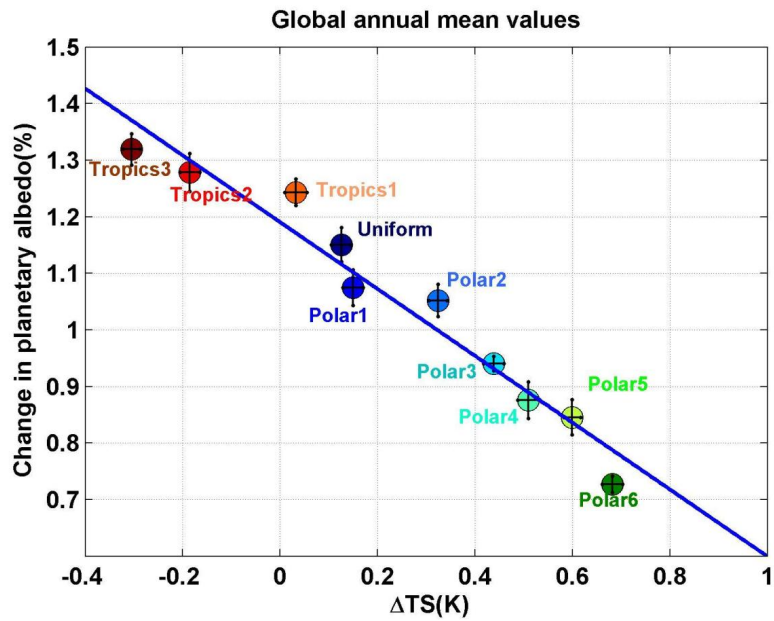
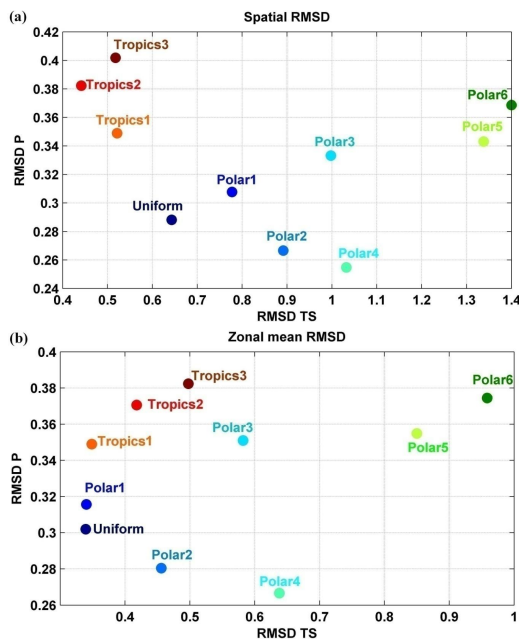


Fig. 2. Change in planetary albedo in fixed-SST vs. surface temperature change in slab ocean geoengineering simulations. The radiative forcing associated with albedo changes drive the temperature changes. Polar cases have lower albedo changes relative to the uniform case and hence are warmer and wetter while opposite is true for Tropics cases. The horizontal and vertical bars represent the standard error of the respective variables; temperature standard errors are calculated from the last 30 yr of 60 yr SOM simulations while albedo standard errors are calculated from the last 20 yr of 30 yr fixed-SST simulations.

25405



25406

Fig. 3. Root mean square difference (RMSD) of surface temperature and precipitation between geoengineering and control simulation normalized by spatial standard deviation in the control scenario computed for the global domain (top panel) and for the zonal averages (bottom panel). The annual means of the last 30 yr of the 60 yr control simulation are used to estimate the standard deviation. Simulation nearest to x axis represents the best precipitation mitigating scenario while the one closest to y axis represents the best surface temperature mitigating scenario. Scenarios with maximum aerosol concentrations at the poles have larger RMSD in temperature and conversely simulations with maximum at the equator have larger RMSD in precipitation.

25407

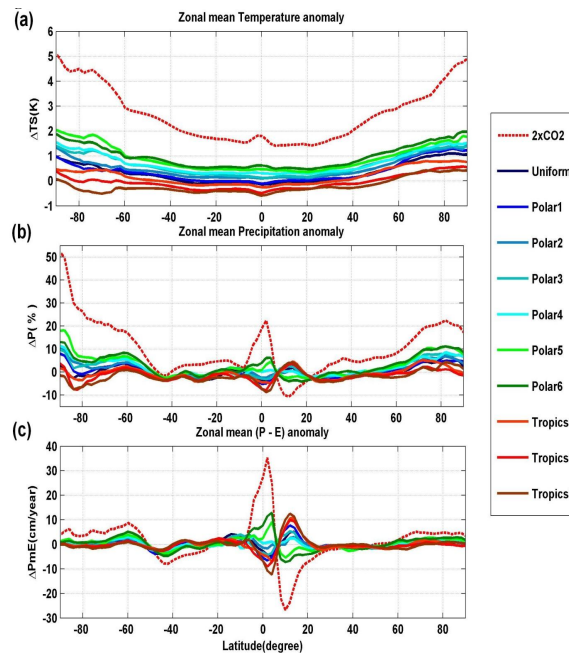


Fig. 4. Zonal means of change in surface temperature (ΔTS), precipitation (ΔP) and precipitation minus evaporation (ΔPmE). **(a)** Zonal mean ΔTS increases monotonically with increase in maximum concentrations over the poles and decreases with increase in tropical maxima. **(b)** Zonal mean ΔP : polar maximum causes enhanced precipitation. **(c)** Zonal mean ΔPmE : polar maximum causes enhanced precipitation minus evaporation. Results shown are averages of the last 30 yr of 60 yr simulations.

25408

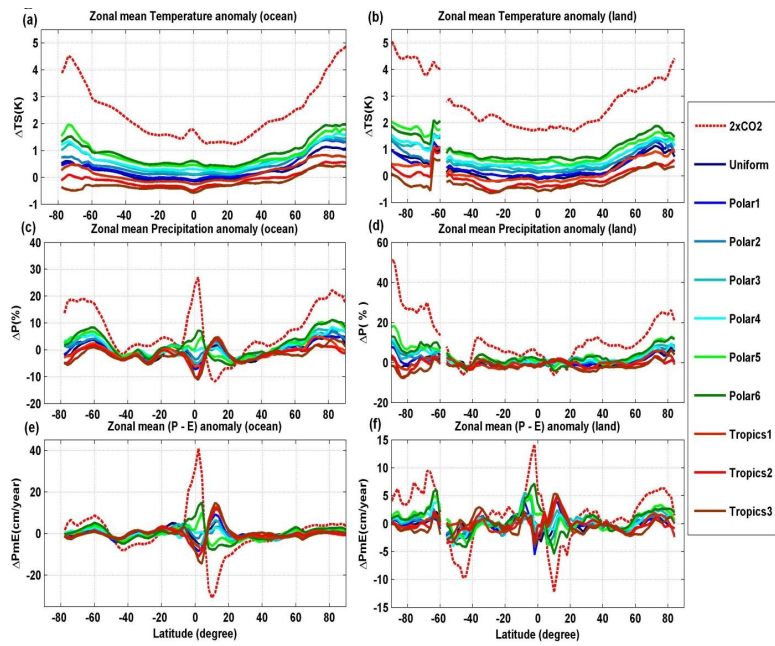


Fig. 5. Changes in zonal mean surface temperature (ΔTS), precipitation (ΔP) and precipitation minus evaporation (ΔPmE) over ocean (left panels) and land (right panels). **(a, b)** Zonal mean ΔTS increases monotonically with increase in the magnitude of maximum concentration of aerosols over poles and decreases with increase in the magnitude of tropical maximum. **(c, d)** Polar maximum causes enhanced precipitation. **(e, f)** Polar maximum causes enhanced precipitation minus evaporation. Results shown are averages of the last 30 yr of 60 yr simulations.

25409

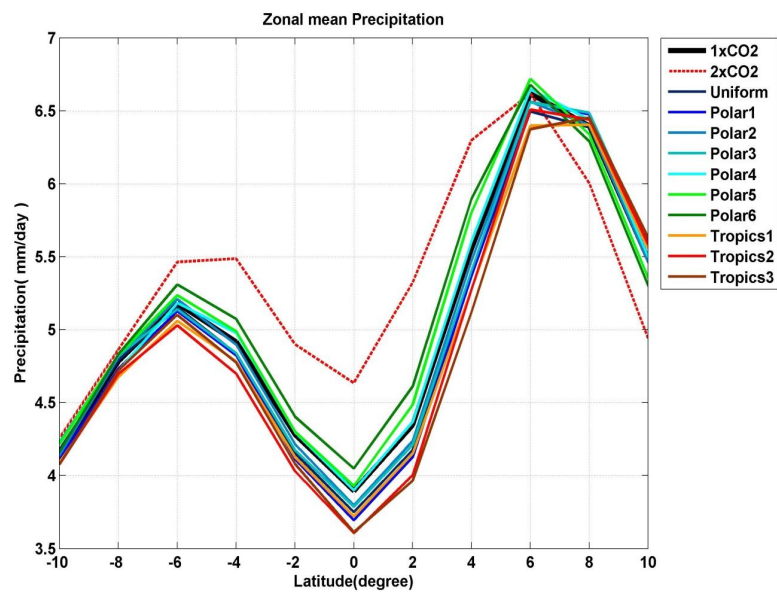


Fig. 6. Zonal mean precipitation over the globe. The position of intertropical convergence zone (ITCZ) remains the same in all the geoengineering cases. The zonal mean precipitation decreases monotonically over the equator as the global mean radiative forcing increases. Results shown are averages of the last 30 yr of 60 yr simulations.

25410

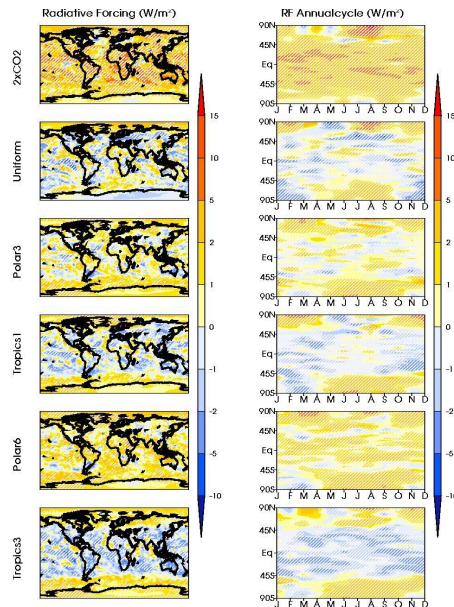


Fig. 7. Spatial pattern of radiative forcing (left panels) and the seasonal cycle of radiative forcing (right panels) in the $2 \times \text{CO}_2$, uniform, and some Polar and Tropics geoengineering scenarios. In the Uniform and Tropical cases, there is a residual positive forcing in the high latitudes and negative forcing in the low latitudes indicating an inexact compensation. The residual seasonal cycle is clearly visible in the polar regions in the Uniform case while in the Polar3 and Tropics1 cases the residual seasonal cycle has a much smaller strength. Hatching indicates the region where the changes are significant at 1% level. Significance level was estimated by Student t test. Results shown are averages of the last 20 yr of 30 yr simulations with fixed sea surface temperature and sea ice fraction.

25411

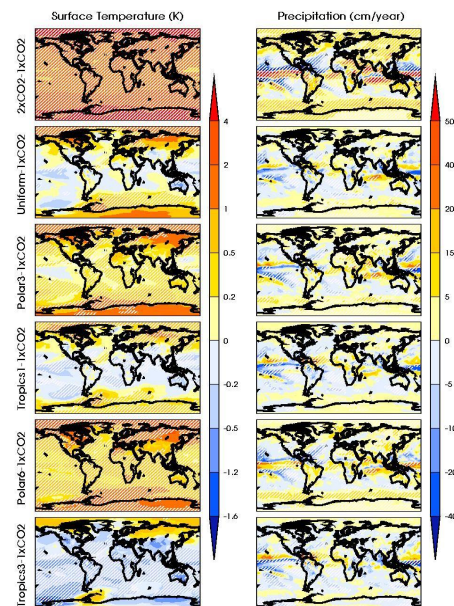


Fig. 8. Changes in annual-mean surface temperature (left panels) and precipitation (right panels) in the $2 \times \text{CO}_2$, uniform, and some Polar and Tropics geoengineering scenarios relative to the control ($1 \times \text{CO}_2$). Hatching indicates the region where the changes are significant at 1% level. Significance level was estimated using Student t test. Both surface temperature and precipitation changes are large and significant everywhere in the $2 \times \text{CO}_2$ and extreme scenarios (Polar6 and Tropics3). Although significant over large regions, both temperature and precipitation changes are small in the Uniform case. Polar3 scenario mitigates global mean precipitation but not global mean temperature while Tropics1 scenario mitigates global mean temperature but with reduced precipitation. Results shown are averages of the last 30 yr of 60 yr simulations.

25412

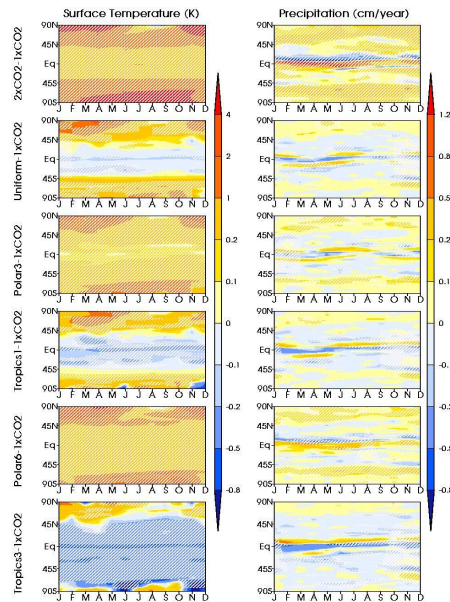


Fig. 9. Seasonal cycle of the changes in the zonally averaged surface temperature (left panels) and precipitation (right panels) in the $2 \times \text{CO}_2$, uniform and some Polar and Tropics geoengineering scenarios relative to the control ($1 \times \text{CO}_2$). Seasonal variations in temperature response mostly occur in the high latitudes with larger warming in the winter and weaker warming in the summer. Hatching indicates the region where the changes are significant at 1% level. Significance level was estimated by Student t test. In case of surface temperature, the change in seasonal cycle is significant for both the Polar cases. Results shown are averages of the last 30 yr of 60 yr simulations.

25413

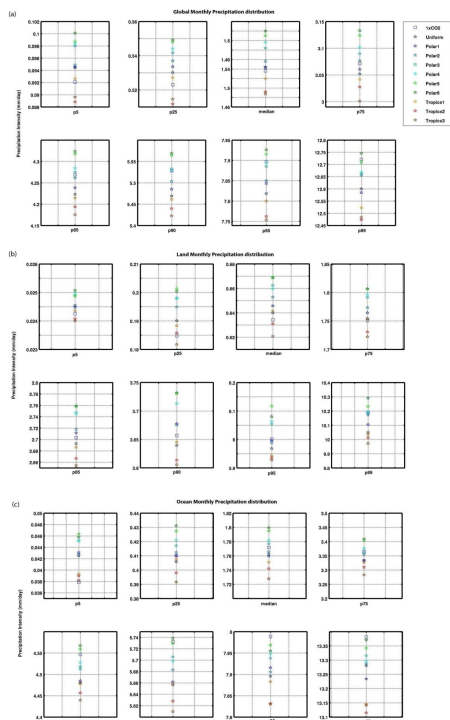


Fig. 10. Percentile values (p5, p25, median, p75, p85, p90, p95 and p99) of precipitation intensity over (a) Globe, (b) Land, (c) Ocean. There is a monotonic increase in precipitation for all percentile values as the maximum concentration of aerosols over poles increases. Grid-level monthly mean precipitation are used to calculate the percentile values. The last 30 yr of 60 yr simulations are used for the statistics.

25414

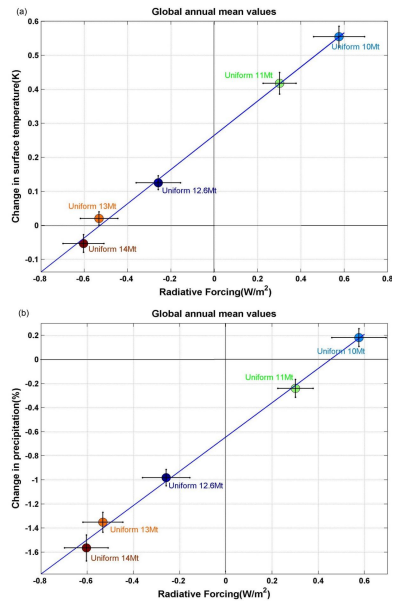


Fig. 11. (a) Radiative forcing (RF) vs. surface temperature change. **(b)** Radiative forcing vs. % precipitation change for uniform distribution scenarios with 10 Mt, 11 Mt, 12.6 Mt, 13 Mt and 14 Mt. More aerosol mass leads to negative residual radiative forcing and hence cooler and drier climate, and smaller aerosol mass leads to positive residual radiative forcing and hence warmer and wetter climate. In **(a)** and **(b)** the horizontal and vertical bars represent the standard error of the respective variables. Results shown are averages of the last 20 yr of 50 yr SOM simulations for temperature and precipitation while the last 20 yr of 40 yr fixed-SST simulations are used for radiative forcing calculations.